JOURNAL OF THE EXPERIMENTAL ANALYSIS OF BEHAVIOR 2002, **77,** 105–124 NUMBER 1 (JANUARY)

A TUNED-TRACE THEORY OF INTERVAL-TIMING DYNAMICS

J. E. R. STADDON, I. M. CHELARU, AND J. J. HIGA

DUKE UNIVERSITY AND
TEXAS CHRISTIAN UNIVERSITY

Animals on interval schedules of reinforcement can rapidly adjust a temporal dependent variable, such as wait time, to changes in the prevailing interreinforcement interval. We describe data on the effects of impulse, step, sine-cyclic, and variable-interval schedules and show that they can be explained by a tuned-trace timing model with a one-back threshold-setting rule. The model can also explain steady-state timing properties such as proportional and Weber law timing and the effects of reinforcement magnitude. The model assumes that food reinforcers and other time markers have a decaying effect (trace) with properties that can be derived from the rate-sensitive property of habituation (the multiple-time-scale model). In timing experiments, response threshold is determined by the trace value at the time of the most recent reinforcement. The model provides a partial account for the learning of multiple intervals, but does not account for scalloping and other postpause features of responding on interval schedules and has some problems with square-wave schedules.

Key words: interval timing, multiple time scale, scalar timing, memory, habituation, pigeons, rats

Humans and animals can readily learn to anticipate the time when a reinforcing event will occur. This process is termed *interval timing*. It is typically studied in well-trained animals under steady-state conditions where it is characterized by two properties: (a) The temporal dependent variable—*wait time* (pause) on fixed-interval (FI) reinforcement schedules, the average time of maximal responding (peak time) on the peak-interval procedure—is typically proportional to the to-be-timed interval (*proportional timing*). (b) The standard deviation of the temporal measure is proportional to its mean. This is termed *scalar* or *Weber law* timing (Dews, 1970; Gibbon, 1977; Staddon, 1965). Neither property holds for every temporal schedule or temporal dependent measure (Staddon & Higa, 1999; Zeiler & Powell, 1994), but for certain standard situations these two properties are reliably found.

It was for many years assumed that interval timing requires much training—experience with tens or even hundreds of intervals—before the two properties emerge. But Wynne and Staddon (1988) showed that pigeons could adapt rapidly to changing time to reinforcement. For example, one series of experiments used the *response-initiated delay* (RID) schedule illustrated in Figure 1: After food reinforcement, the animal is free to make the operant response, a key peck, at any time. Let us say that it responds after waiting a time t s. This initiates an experimenter-controlled clock that runs for a further time, T, at the end of which another food reinforcement is delivered. In two experiments, Wynne and Staddon exposed pigeons to various versions of this procedure, including one in which the independent variable was $t + T$, and found a simple invariant relation: Time to first response (wait time) is linearly related to the time between food deliveries (interreinforcement interval, IRI, in this case equal to $t + T$) (i.e., proportional timing). Moreover, the slope of this function was the same whether the average IRI varied from day to day or changed only after several days at each value. In a third experiment, using a positive feedback procedure, they confirmed the inference that pigeons can adjust their wait time rapidly in response to changes in IRI.

The most direct test of the idea that a change in IRI has an immediate effect on the succeeding wait time is to present unpredictably a single short (or long) IRI in a series of constant longer (or shorter) IRIs. Higa and Staddon used this impulse procedure in a series of studies (e.g., Higa, 1996; Higa, Wynne, & Staddon, 1991; Staddon, Wynne, & Higa, 1991). A typical result is shown in Figure 2. The data are striking: The effect of a short

This research was supported by grants from NIMH and NIDA to Duke University.

Correspondence should be addressed to J. E. R. Staddon, Department of Psychology and Brain Science, Duke University, Durham, North Carolina 27708 (E-mail: staddon@psych.duke.edu).

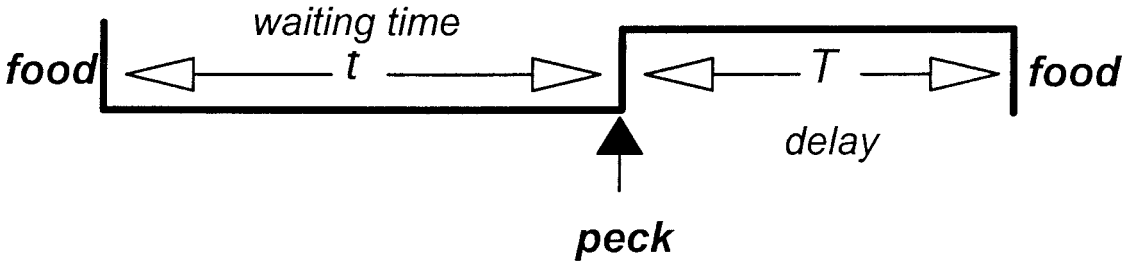

Fig. 1. One cycle of an RID schedule. The organism waits a time t before making the first operant response, which initiates a schedule-controlled time T that terminates with food reinforcement. In most of our experiments T was set so that $t + T$ (the interfood interval) was the manipulated variable.

IRI interpolated into a series of longer IRIs is to shorten the wait time in the following IRI, and only in the following IRI. This effect occurs, with only slight variations, when several impulse intervals, closely or widely spaced, are presented, as we illustrate in a moment.

Two other dynamic schedules are the step (up or down) and cyclic. Step schedules resemble impulse schedules in that the prevailing IRI changes up or down at a random point in the experimental session. The difference is that on step schedules it stays changed until the end of the session rather than reverting to the baseline value after just one IRI. On cyclic schedules the IRI changes progressively up and down, according to a sine or other periodic function. Performance on the cyclic schedule usually follows the impulse pattern: Wait time is proportional to the preceding IRI (one-back tracking). But on step schedules, the effect of the change takes a few IRIs to settle down, more on step up than step down. The relatively slow adjustment to step-up schedules may account for the fact that the effect of single long impulse intervals is much less than the effect of single short intervals. Lejeune, Ferrara, Simons, and Wearden (1997) and Church and Lacourse (1998) have reported similar results in experiments with the peak-interval procedure and progressive-interval schedules.

Variable-interval (VI) schedules yield apparently anomalous data. Wait times are very short, and no one seems to have published data showing a significant correlation between wait time and the duration of the previous IRI, even though IRI durations on VI typically vary over a wide range.

THEORY

What is the process that underlies these dynamic effects? Numerous theories of steady-state interval timing have been proposed, but only three attempts seem to have been made to explain the effects we have just described. Machado (1997; see also Higa & Staddon, 1997) explored the dynamic implications of a sequential-state model similar to the behavioral theory of timing proposed by Killeen and Fetterman (1988). Machado showed that given appropriate values for a learning-rate parameter, α, the effect of a single IRI might dissipate rapidly, so that his model could simulate the one-back tracking result of the impulse experiment. However, because Machado's main focus was on acquisition curves for standard temporal schedules and steady-state data for the learning of multiple intervals, he did not attempt to account for the other dynamic results we have described.

Staddon and Higa (1991) and Higa and Staddon (1997; see also Staddon, 2001) studied a diffusion-based model for temporal dynamics (the diffusion-generalization model). The idea of this model is that time is represented spatially. The occurrence of reinforcement increments activation at a point whose distance from the origin is proportional to time elapsed since the time marker (reinforcer delivery, on fixed-interval [FI] and RID schedules). Activation diffuses constantly in real time. Response rate is represented by the height of the activation surface at each instant of time within the to-be-timed interval. This rather cumbersome model can simulate steady-state results from procedures that require the organism to learn about two or more intervals, such as mixed FI x FI y sched-

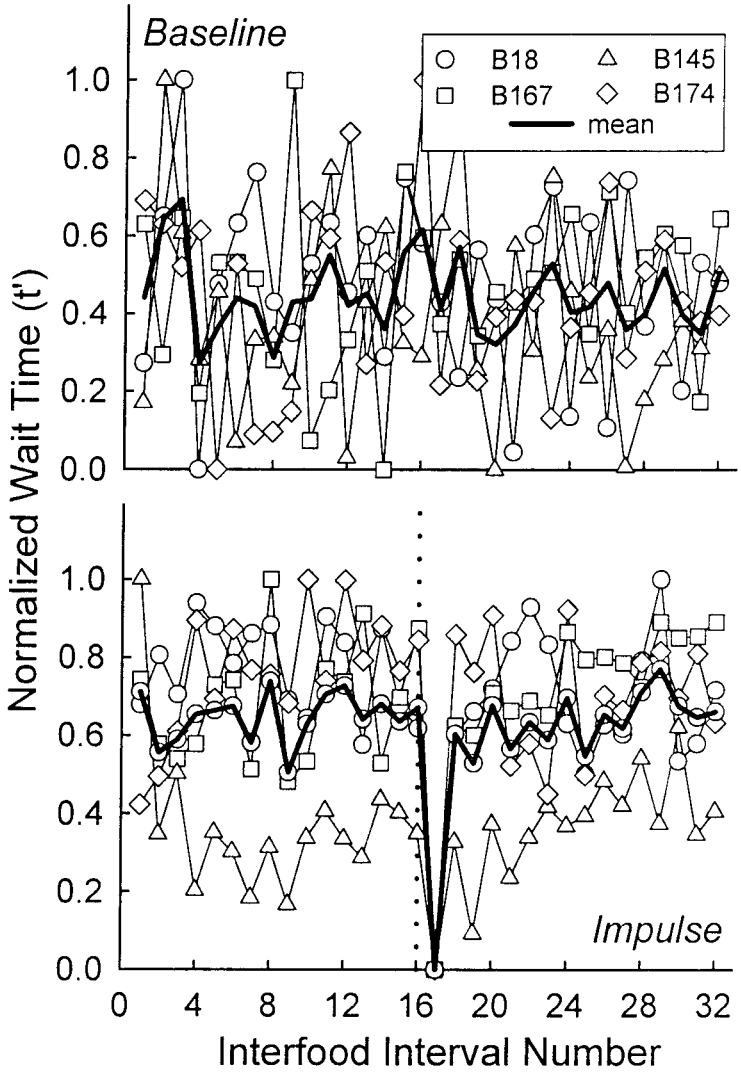

Fig. 2. Top: heavy line: normalized average wait time, $WT_{norm} = (WT - WT_{min})/(WT_{max} - WT_{min})$, during a randomly selected 32-interval period during the baseline RID 15-s condition (10 sessions). Light lines, open symbols: data for 4 individual pigeons. Bottom: similar data during the impulse condition, in which a single 5-s IRI occurred at a random point once per session. The location of the 5-s interval is shown by the dashed vertical line, and the points to left and right are the data from the 15 preceding and following intervals (from Higa & Staddon, 1997, Figure 3).

ules, as well as data from step-up and step-down experiments (Figure 3). The diffusion-generalization model cannot duplicate the data from cyclic schedules, however. Rather than simply tracking the input cycle with a lag of one interval, the model yields a skewed output that sometimes lags the input by several intervals.

Wynne and Staddon (1988) proposed a simple model that nevertheless does about as well as any other with these dynamic data. *Linear waiting* is the idea that the wait time in IRI $N + 1$ is simply a linear function of the preceding IRI N. For RID schedules, this amounts to the following relation:

$$t_{N+1} = a(t_N + T_N) + b, \qquad 0 < a < 1, \quad (1)$$

where t_N is wait time in interval N, T_N is delay in interval N, and a and b are constants; b is generally close to zero. Obviously this model

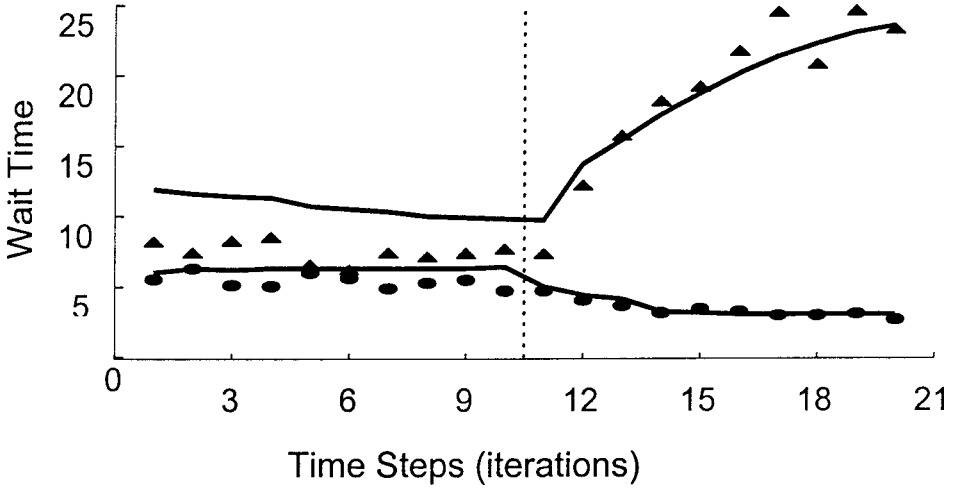

Fig. 3. Average data from a step experiment simulated by the diffusion-generalization model (from Higa & Staddon, 1997, Figure 11).

can simulate all those data for which wait time is proportional to the preceding IRI, which is to say most of the impulse experiments, sine tracking and step down—but not step up, in which there is typically a substantial lag. However, linear waiting does not duplicate behavior on VI schedules: very short wait times that are essentially uncorrelated with the preceding IRI. The problem seems to be that linear waiting permits no effect of IRIs earlier than the preceding IRI. Yet the lagged effects on step schedules, as well as some effects of daily and longer shifts in schedule parameters (Wynne & Staddon, 1992), show that earlier IRIs do exert some effect on current wait time. Linear waiting also cannot, without additional assumptions, duplicate the Weber law property of timing.

The Multiple-Time-Scale Theory

In this paper we discuss a dynamic model that combines features of linear waiting and the habituation-based multiple-time-scale (MTS) model of interval timing (Staddon & Higa, 1996, 1999). We first show that this model can handle standard steady-state timing data: proportional timing and the Weber law property. We go on to explore its ability to simulate dynamic interval-timing data.

The basis of the MTS theory is simple: (a) An event, such as a time marker in an interval-timing experiment, has an aftereffect. This is usually termed short-term memory, but we have no commitment to that term and it is sometimes inappropriate, in that event aftereffects may sometimes be very persistent. (b) This aftereffect, which we will term a *memory trace,* declines with postevent time according to a negatively accelerated function, rapidly at first, more slowly later. (c) An adequate model for the dynamics of the trace is provided by a chain of thresholded integrators. (d) Wait time is determined by the value of the trace at the time of reinforcement.

The model represented by Properties a through c, plus an additional assumption that response strength is equal to the difference between the direct effect of the stimulus and the remembered effect (trace strength), was first proposed to account for a ubiquitous property of habituation: that habituation after widely spaced stimuli, though weaker than after a closely spaced series, may be more persistent (rate sensitivity; Staddon & Higa, 1996). More recently, we have suggested that the memory-trace component of the MTS habituation model can provide the "clock" for steady-state interval timing (Property d; Staddon, 2001; Staddon & Higa, 1999).

The model. Figure 4 shows how the MTS model works. At the top is a single unit of the system. When a stimulus such as a time marker occurs, the unit gets a brief input that injects a certain amount of integrator activation, $X_1(t)$. In most of our simulations, $X_1(t)$ is set to unity during one time step, corresponding to the occurrence of the time marker (food reinforcement), and is zero at all

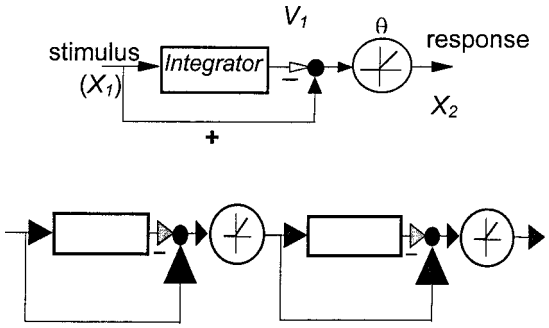

Fig. 4. Top: single-integrator (single-unit) stimulus-type habituation model. Each stimulus, X, increments a leaky integrator. The integrated effects of past stimuli, V_I, are subtracted from the current stimulus, X, and the above-threshold difference, $X - V_I - \theta$, is the response strength V_o. Bottom: two cascaded units; the input to the second is the output of the first. The system output is the output of the last unit in the cascade.

other times. At stimulus offset, the integrator activation decays at a rate determined by its time constant. The equations for the single unit shown at the top of Figure 4 are

$$X_2(t) = \begin{cases} X_1(t) - V_1(t-1), & \text{if } X_2(t) > \theta \\ 0, & \text{otherwise,} \end{cases} \quad (2)$$

$$V_1(t) = a_1 V_1(t-1) + b_1 X_1(t), \qquad 0 < a_1 < 1, \qquad b_1 > 0, \quad (3)$$

where $V_1(t-1)$ is the integrated effect of past stimuli at time $t-1$, $X_2(t)$ is the output at time t, θ is a threshold, a_1 is a discrete-time constant that reflects the period over which past stimuli contribute, $X_1(t)$ is the effect of a stimulus (here, the time marker) at time t, and b_1 is the weighting of the stimulus effect. A nonnegative threshold ($\theta \geq 0$) is necessary to prevent the output, $X_2(t)$, from going negative, which implies unmeasureable negative behavior.

The single-unit system at the top of Figure 4 does *not* show rate sensitivity, because recovery rate (i.e., the decay of V_1 when X_1 is zero) is determined solely by a_1, which is constant and independent of system history. Rate sensitivity requires at least two units in cascade, as in the bottom of Figure 4, with the second time constant, a_2, slower than the first: $a_1 < a_2$. The input to the second unit is just the output of the first. For a multiunit system, the input to each unit is the output of the preceding unit. The inhibitory feedback loop associated with each integrator (Equations 2 and 4, below) means that activation of each integrator reduces the output of each unit, and hence reduces the input to the next unit in line.

The equations for the jth unit of the cascade are

$$X_j(t) = \begin{cases} X_{j-1}(t) - V_{j-1}(t-1), \\ \quad \text{if } X_j(t) > \theta_j \\ 0, \quad \text{otherwise,} \end{cases} \quad (4)$$

$$V_j(t) = a_j V_j(t-1) + b_j X_j(t), \qquad 0 < a_j < 1, \qquad b_j > 0, \quad (5)$$

where V_j is the integrator output of the jth unit in the cascade ($j > 1$), X_{j-1} is the output of the preceding unit, and a_j and b_j are constants. In all simulations, b_j is the same for all units, and a_j is a one-parameter (λ) exponential function of j—so that the number of free parameters is much less than the number of units (see legend to Figure 6 for details).

The output of each unit is thresholded (all thresholds, θ_j, are zero in our simulations), which ensures that units receive an input only when the stimulus, X_1, is present. These pass-through thresholds are essential to the rate-sensitive property of the system. Without them, the system memory (the sum of V values, see below) will always persist longer after massed training than after spaced training. For simulating interval timing over the usual range, a system with eight or more units is necessary. Although the notation we use here is a little different, this part of the model is identical to Staddon and Higa's (1996) MTS habituation model.

The stimulus (X_1) for this system is a psychological variable. Just what physical property of the time marker—its onset or offset, duration, or some combination—corresponds to $X_1(t)$ is something to be discovered empirically. For the predictions we will discuss, all that is necessary is that each occurrence of the time marker (e.g., food reinforcement) has the same effect and that larger reinforcers have larger effects.

Tuned trace. As a model for habituation, this system embodies the idea that the strength of a habituated response is proportional to the strength of the stimulus minus the strength of the memory for the stimulus: Response

equals stimulus minus memory trace. With repeated stimulation, the memory for the stimulus increases (to some asymptote). Habituation occurs because the difference between the memory and the effect of the stimulus is reduced as the strength of the memory trace increases.

The activation levels of the integrators, V_j, correspond to the memory of this system. It is relatively straightforward to show (Equation 2 and Appendix) that with thresholds all equal to zero, the response of an M unit cascade to an input is equal to the stimulus strength $X_1(t)$ minus the sum of the V values. Thus, the value of the memory trace, $v(t)$, of the cascade is simply the sum of the integrator values V_i:

$$v(t) = \sum_{i=1}^{M} V_i(t), \tag{6}$$

where M is the number of integrators in the cascade. It is $v(t)$ that comprises the "clock" in this system.

When the MTS timer is in the steady state with an FI input series, the trace $v(t)$ is a periodic signal, with a period equal to the timing interval T. We show in the Appendix that a cycle of the trace function has the form

$$v(t) = \sum_{i=1}^{M} V_i(T)\, a_i^t, \tag{7}$$

where $V_i(T)$ is activation of integrator i at stimulus offset (i.e., at the beginning of the to-be-timed interval), a_i is the time constant of the ith integrator, and M is the number of integrators in the cascade. Thus the form of the trace is a sum of exponentials. Its form depends not only on the number of integrators and their time constants but also on their activation values when the interval begins (i.e., the initial condition of the system, a vector of M-V values).

The trace $v(t)$ from the cascade of habituation units (i.e., Equations 6 and 7) constitutes a sort of clock. However, the form of the MTS trace is not fixed, but depends on the system history. This is easy to see intuitively. Consider the trace after a series of closely spaced stimuli (time markers). Because the stimuli are closely spaced, the early, fast integrators in the cascade will decay little in between stimuli and so will retain high activation—and will thus reduce the input to later, slower integrators some of which may not be activated at all. When stimuli are no longer presented, the fast integrators early in the cascade (low i values in Equation 6) will have high initial (V_i) values compared to the later, slower integrators. Hence, the trace (Equation 6) will decay rapidly, and the real time to reach a fixed threshold will be short. Conversely, after a training series of widely spaced stimuli, early, fast integrators will lose activation between stimuli, allowing input to the later, slower integrators, which will tend to dominate, and the trace will decay slowly. Hence, the time to reach the same fixed threshold will be longer. MTS is thus a tuned trace model. The decay rate of the trace, which is determined by the weights $V_i(T)$ in Equation 6, is tuned by the past history of the system: fast after a massed training series, slow after a spaced series (see, e.g., Staddon, Higa, & Chelaru, 1999, Figure 1). The exact values for $V_i(T)$, in the case of an FI schedule, are computed in the Appendix.

Response rule. The simplest way to use the trace as a timer is via a response threshold. The value of the trace, v, is monotonically related to time, so that a fixed response threshold will initiate responding at the same time, so long as v decays in the same way after each occurrence of the time marker. The question for a dynamic model is, how is the threshold set?

We have found that the simplest rule seems to be the best. The response threshold, φ, is set by each occurrence of reinforcement as follows:

$$\varphi(N) = v_{\mathrm{rft}}(N-1) + \xi X(N), \tag{8}$$

where N is the IRI number, $X(N)$ is the reinforcement magnitude at the beginning of the current IRI, $v_{\mathrm{rft}}(N-1)$ is the trace value at the end of the preceding interval (i.e., at the moment just before reinforcement), and ξ is a constant. In words, the system remembers the value of the declining trace at the instant of each reinforcement [reinforcement memory: $RFM(N) = v_{\mathrm{rft}}(N-1)$, see the Appendix], and begins responding when the trace declines to that value plus a constant increment, ξ, scaled to the prevailing reinforcement magnitude.

Notice that this rule means the threshold is set by each reinforcement (as in linear waiting). But, unlike linear waiting, this model

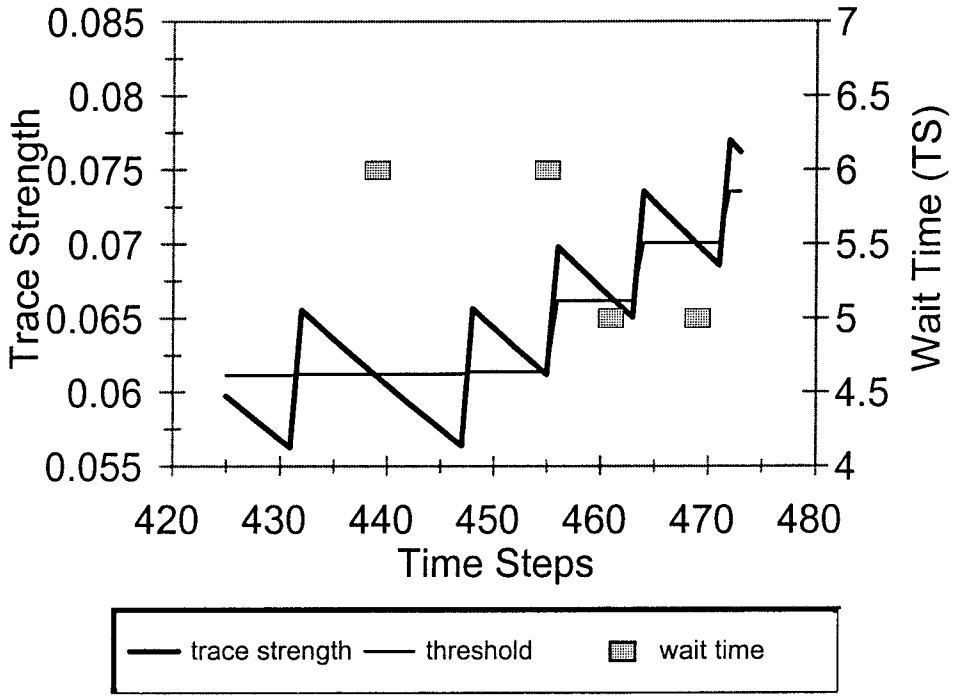

Fig. 5. Response rule for the MTS timing model. Heavy line: trace strength during a sequence of two long (16 time steps) followed by two short (8 time steps) IRIs. Up-spikes indicate reinforcements. Light line: response threshold, set to a constant plus the value of the trace at the preceding reinforcement (reinforcement memory: RFM; see Appendix). Gray squares: wait time in the four intervals (right *y* axis). Wait time adjusts immediately following the long-short transition.

does not imply instantaneous adaptation to any new to-be-timed interval—because the tuning of the trace is *not* instantaneous. It takes several intervals—more following an upshift (short → long) than a downshift—following the transition from one interval value to another before the trace settles down to its new form. Thus, the MTS timing model incorporates both a fast and a slow process, although these do not correspond in any simple way to the conventional cognitive idea of short- and long-term memory "stores."

Figure 5 shows the relations among trace strength (zigzag line: left *y* axis), threshold (step function), and time to first response (wait time: intersection of threshold and trace lines; the value is plotted on the right *y* axis, gray squares) before and after the transition from a long to a short IRI. For the first two IRIs the wait time is relatively long (first two squares), but as soon as the prevailing IRI shortens, the threshold shifts and wait time decreases (last two squares).

SIMULATIONS

Steady State

The steady-state properties of this model follow from the steady-state form of the trace. A compact way to represent the steady-state trace after training under different fixed intervals is shown in Panel 2 of Figure 6, which shows traces normalized as a proportion of the prevailing IRI along the time axis and displaced along the *y* axis by an amount v_{rft} so that all are zero at the time of reinforcement (end of the to-be-timed interval). The constant threshold in Equation 8 corresponds to a horizontal line in this plot (dashed line). The figure shows steady-state traces after extended training at three IRIs over the range of 10 to 600 time steps. Each trace decays at a rate appropriate to its training IRI: slowly after 600 time-step training and rapidly after 10 time-step training, so that the normalized traces more or less superimpose over most of the range. Because the traces are close to-

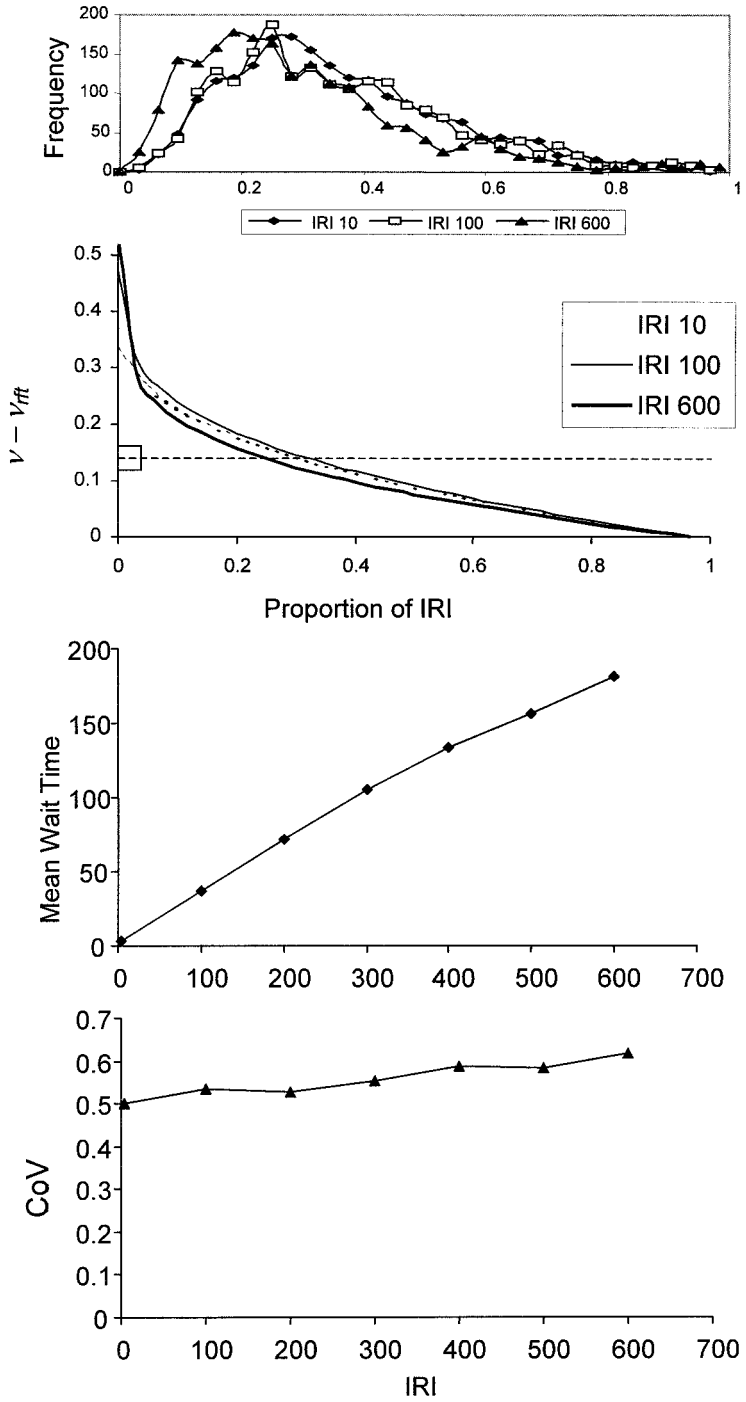

Fig. 6. Steady-state properties predicted by the MTS timing model with threshold noise. Top: wait-time distributions for three IRIs, plotted as a proportion of the IRI (x axis). Panel 2: steady-state traces for three IRIs plotted as a proportion of the training IRI and translated along the y axis so that v_{rft} is zero for all (Point 1,0). Horizontal dashed line indicates the response threshold. The rectangle on the left indicates the noise distribution added to the threshold (Equation 9) to produce the distributions in the top panel. Panel 3: mean wait time for IRIs ranging from 10 to 600 time steps. Bottom: coefficient of variation (CoV) for steady-state wait-time distributions from IRIs of 10 to 600 time steps. All curves were generated by the same 14-unit model with $X_1(t) = 1$, $a_j = 1 - e^{-\lambda j}$ and $\lambda = .675$, $b_j = .04$, $\xi = .14$, and $\eta = .04$.

gether in the region of the threshold, the model yields a wait time that is proportional to the IRI: proportional timing (shown in the third panel).

The three distributions at the top of Figure 6 show the effect of adding a small rectangular noise term, ϵ, with a mean of zero and unit range with multiplier $\eta = .04$, to the threshold (rectangle on the y axis on the threshold line in Panel 2 in Figure 6):

$$\varphi(N) = \nu_{\text{rft}}(N - 1) + \xi X(N) + \eta\epsilon(t). \quad (9)$$

Equation 9 is just Equation 8 with an added noise term. We used this model for all the simulations that follow. With the addition of threshold noise, variability (standard deviation) in wait time is approximately proportional to the mean wait time (i.e., an approximately constant coefficient of variation, CoV), which is the condition for Weber law or scalar timing, shown in the bottom panel for a range of training intervals from 10 to 600 time steps. Because the trace in the region of the threshold is not perfectly linear, symmetrical threshold variation yields a slightly asymmetrical wait-time distribution (top panel) in accordance with data (e.g., Church, Meck, & Gibbon, 1994; Wynne & Staddon, 1988). Thus, this model duplicates the most basic steady-state properties of interval timing: proportional timing, Weber law timing, and a right-skewed distribution of wait times.

Reinforcement-magnitude effects. Most clock models for timing separate the timing function, the clock, from the process that starts and stops the clock. But in the MTS timing theory, the two are not separable. If the clock is just memory for the time marker, then different time markers should have different effects. "Time" should appear to flow faster or slower depending on the memorability of the time marker. In all the experiments we discuss here, food delivery—the reinforcer—is the time marker. Small reinforcers are, by many measures, less memorable than large ones, so we may expect the MTS model to predict timing differences when reinforcer magnitude is varied.

In fact, the predicted effects of varying reinforcer magnitude depend on exactly how—over what period of time—it is varied. The steady-state behavior of the model is independent of reinforcement magnitude, so long as

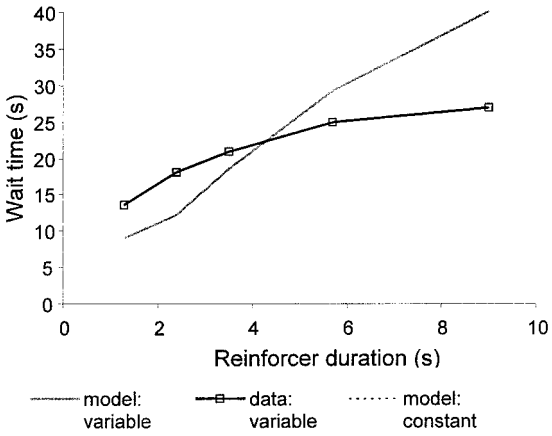

Fig. 7. The effect of reinforcement magnitude on wait time on an FI schedule. Heavy solid line, open squares: data from well-trained pigeons on an FI 60-s schedule, with five different reinforcement durations intermixed in each daily session (L. Talton, unpublished data). Gray line: model, intermixed durations. Dashed line: model, steady-state wait time at each of five reinforcement magnitudes. Model parameters as in Figure 6.

it is constant. In the dynamic simulations we discuss in a moment, $X(t)$ equals 1 (reinforcement) or 0 (the time steps between reinforcers), but the results would be the same for any constant value of $X(t)$. By Equation 8, the response threshold is set relative to the magnitude of the most recent reinforced trace value, ν_{rft}, whatever that may be. So if the trace is the same from interval to interval (as it will be if both interval duration and reinforcer magnitude are constant), wait time will also be the same, because trace shape is always the same under these conditions (Figure 6). This prediction (Figure 7, dashed line) conforms to data: Wait time on FI schedules is essentially independent of reinforcement magnitude in the steady state (cf. Hatten & Shull, 1983; Lowe, Davey, & Harzem, 1974; Meltzer & Brahlek, 1970).

But if different magnitudes are intermixed interval by interval, then even in the steady state, wait time is longer following longer (larger) reinforcers (Staddon, 1970). This result is also predicted by the model. Moreover, as in the data, the effect is due more to shortening of wait time after shorter-than-average reinforcers than to lengthening after long ones. The effect of a ninefold change in reinforcer amount (duration) is similar to results from pigeons. Figure 7 shows predictions of the model compared

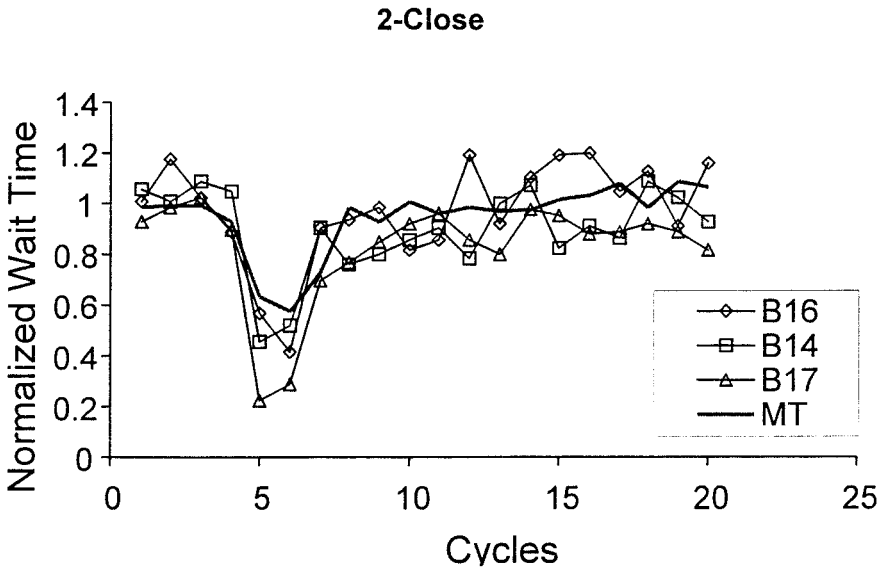

Fig. 8. Response of the model to two impulse intervals. The baseline was an RID schedule with $t + T = 45$ s. Data (light lines with markers) are 10-day average normalized wait times of 3 individual well-trained pigeons in 20 successive IRIs aligned at the two impulse intervals. The two 15-s impulse IRIs occurred randomly in each experimental session against a background of 45-s IRIs. The heavy solid line is the prediction of the 14-unit MTS model described in Figure 6.

with unpublished data from our laboratory (see also Staddon, 1970): Both curves (data: variable; model: variable) have a positive slope, but the model effect is larger. That the model predicts the difference between the constant and variable conditions is probably more significant than the quantitative difference between model and data in the variable condition, which might well be attributable to a nonlinear relation between measured reinforcer magnitude and the input variable, X_1, of the model (cf. Epstein, 1981, 1985). Doubling reinforcer magnitude may less than double X_1, so that assuming proportionality between X_1 and reinforcer magnitude causes the model to overestimate reinforcement-magnitude effects.

This model is not designed to deal with concurrent timing of multiple intervals. However, when noise is added to the threshold (Equation 9) and responding is assumed to continue at a steady rate after the first response in each interval, averaged steady-state performance on a mixed FI *x* FI *y* does show two peaks. But the details of the bimodal response distribution do not conform closely to published data (e.g., Catania & Reynolds, 1968).

Dynamics

If we wish to model dynamics, then the appropriate comparison is with data from individual organisms, because averaging across organisms that may differ in the temporal details of their responses to transient inputs can produce an average that is unrepresentative of any individual, even though the temporal response pattern may be similar across individuals.

Figure 8 shows data from 3 pigeons exposed to a 45-s baseline RID schedule with two shorter (15-s) IRIs presented at a random point in each session. Records from each session were aligned at the two probe intervals (Cycles 4 and 5), and the wait times in each interval were averaged for each animal (light lines with markers). The heavy line (MTS) shows the response of the 14-unit model that generated the traces in Figure 6. The model shows a slightly larger drop in wait time to the second of the two short intervals, but otherwise model and data are similar.

This pattern is continued for six other dynamic schedules in Figures 9 and 10. In each case, the model (with the same parameters as before) duplicates the pattern shown by in-

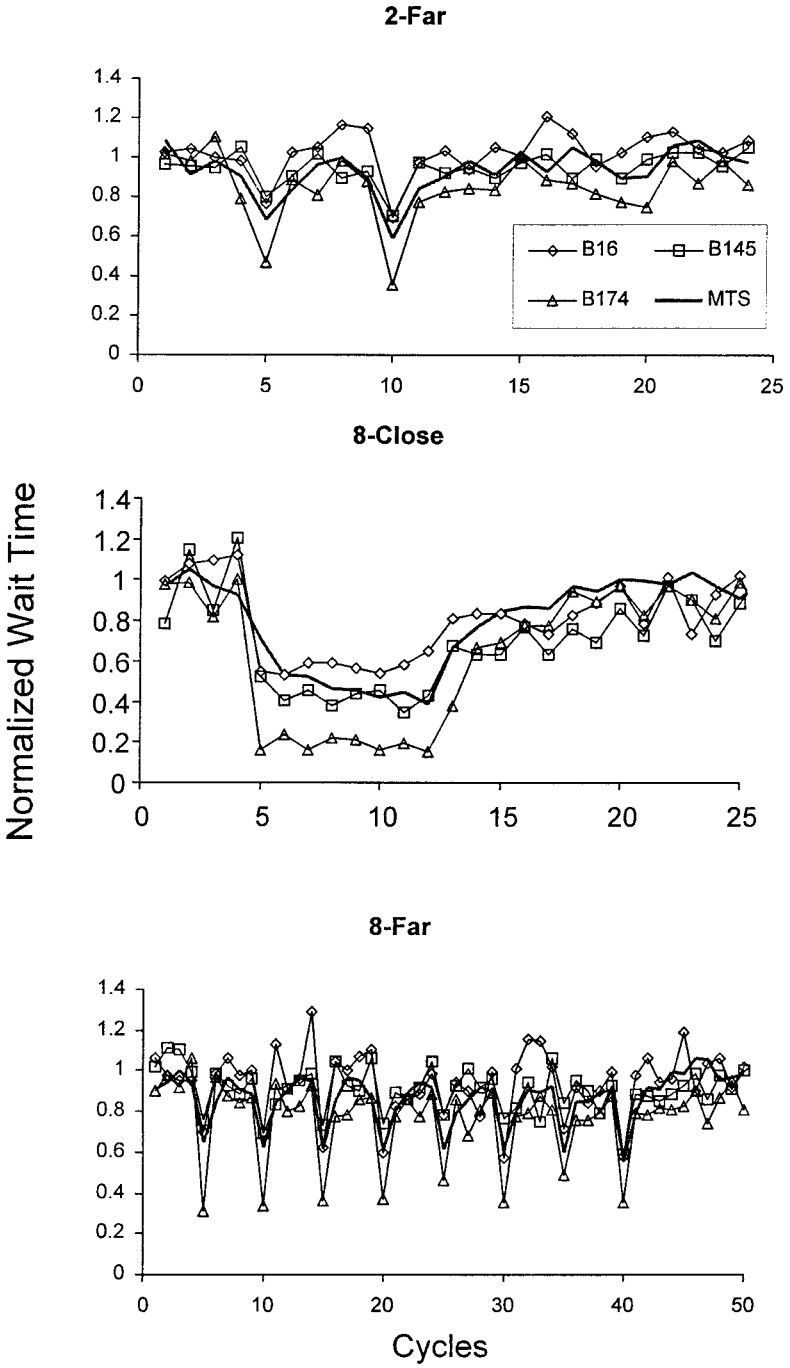

Fig. 9. Response of the model to three impulse patterns. Top: two short (15-s) IRIs separated by eight baseline (45-s) IRIs. Middle: eight short IRIs. Bottom: eight short separated by four baseline IRIs. Light lines + markers: data from 3 individual pigeons. Heavy line: predictions of the MTS model described in Figure 6.

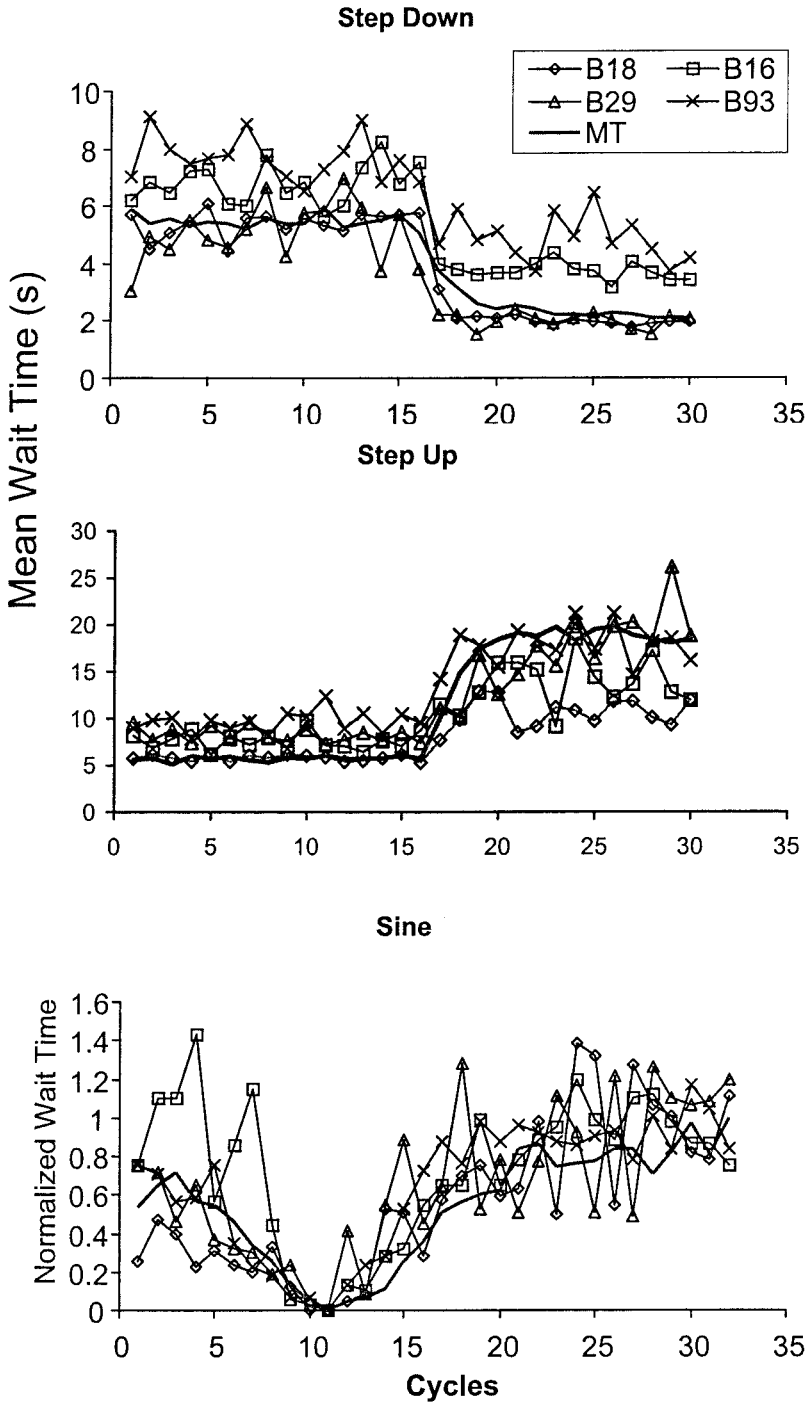

Fig. 10. Response of the model to three impulse patterns. Top: step-down, from 15 s to 5 s. Middle: step-up, from a 15-s IRI baseline to 45 s. Bottom: a single sinusoidal cycle. Light lines: data from 3 individual pigeons. Heavy line: predictions of the MTS model. Light lines + markers: data from 4 individual pigeons. Parameters and other details as in Figure 6.

dividual pigeons. Note that the model duplicates the gradual increase in waiting time shown by the data following the upshift in the eight-close schedule (middle panel, Figure 9). The model also matches the gradual up-and-down changes in the step-up and step-down schedules (top two panels of Figure 10). These gradual changes cannot be duplicated by linear waiting. Finally, note that the model matches the tracking of the sine input pattern shown at the bottom of Figure 10, which cannot be duplicated by the diffusion-generalization model.

In every figure, the MTS model resembles the behavior of individual animals, not group averages. The plotted data are also close to raw observations: Each plotted data point is the average of just 10 individual observations. We have not yet looked into fitting the model to data from individual animals, but the problem is clear in outline. For simplicity, in all our simulations we held parameter b_i in Equations 3 and 5 constant and equal to .04. The effect of varying this parameter is mostly to change the scale of the trace, that is, an approximately proportional effect on the absolute value and relatively little effect on proportional change caused by each reinforcer. Parameter λ, on the other hand, determines the relative importance of the fast (low j) or slow integrators in the chain. For example, with $\lambda = 0.2$, the first three a values are .1813, .3297, and .3412, whereas with $\lambda = 0.8$ they are .5507, .7981, and .9093. The second system will take longer to stabilize and will recover more slowly after extended training than the first. Our impression is that, overall, the system is relatively insensitive to changes in parameters b and λ, especially if the chain is long (i.e., more than 8 or 10 units).

Figure 11 (top) shows the response of the model to a random VI schedule. Light lines show successive IRIs; the heavy gray line at the bottom shows the wait times predicted by the MTS model. The relation between mean wait time and VI value is shown for a range of VI values in Figure 12. As VI duration increases, mean wait time increases to an asymptote of about eight time steps, for VI values ranging from 50 to 200 time steps. Wait time predicted by the model is short, but not as short as available data, which is on the order of 1 to 2 s rather than 5 to 7 s over this range (Baum, 1993, Figure 6). The model predicts that wait time is essentially independent of VI value over much of the range that is similar to the data, which show that "[wait time] increases with interreinforcer interval in a roughly linear fashion, but with a slope far less than 1.0" (Baum, 1993, p. 252).

In the absence of threshold noise ($\eta = 0$ in Equation 9), the predicted correlation between IRI N and the succeeding wait time $N + 1$ is positive, .92, slightly less than 1, which would be the value predicted by linear waiting. (The reason this model differs from linear waiting is that the trace is not identical from interval to interval, but changes according to the recent system history.) The bottom panel of Figure 11 shows the relation with noise (ϵ, with a mean of 0 and a range of .04, the values used in all other simulations) added to the threshold. The correlation between IRI N and wait time $N + 1$ drops from .92 to .34. We have not been able to find published data with which to compare this correlation, but in an unpublished study, J. J. Higa (personal communication, July 18, 2001) presented pigeons with two random-interval schedules (RI 15 s and RI 60 s) for 10 days in a counterbalanced order, and found correlations between obtained IRI (the results for schedule IRI are similar) in interval N and wait time in interval $N + 1$ ranging from .037 to .108 (RI 15 s) and from .002 to .113 (RI 60 s). The correlation with obtained IRIs ranged from .038 to .134 (RI 15 s) and from .011 to .058 (RI 60 s). None of these is significantly different from zero. The correlations predicted by the MTS model, though small and much lower than those predicted by linear waiting, seem to be somewhat higher than those actually observed on random VI schedules.

CONCLUSION

The tuned-trace MTS timing model, combined with a one-back response threshold-setting rule, can duplicate the main properties of rapid timing effects on interval schedules as well as the major steady-state effects such as proportional and scalar timing, skewed wait-time distributions, and the effects of variable reinforcer magnitude. It also simulates the short wait times and absence of temporal tracking on random VI schedules, although empirical IRI versus wait-time correlations are

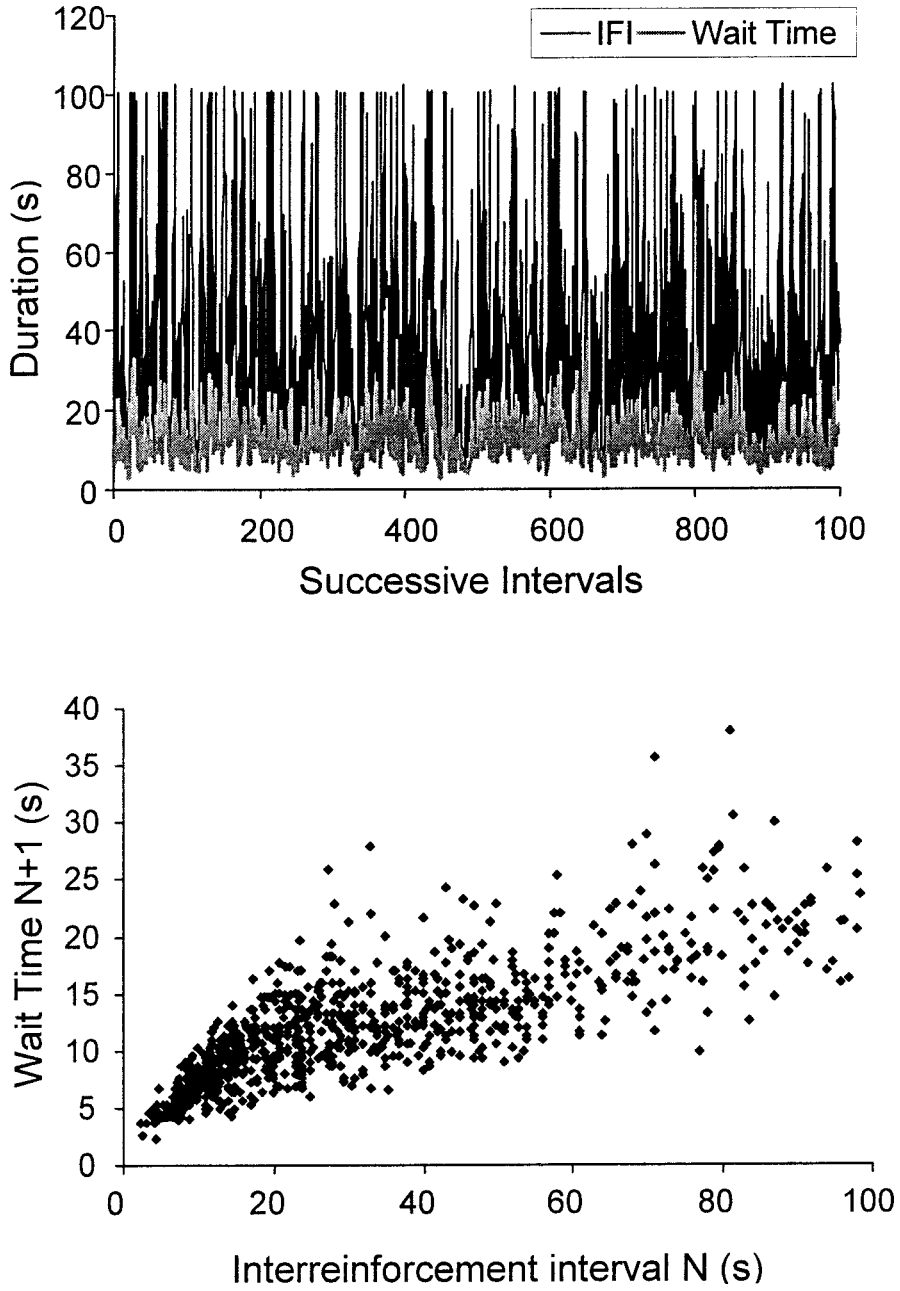

Fig. 11. Top: light line: successive IRIs on a random VI schedule. Heavy gray line: wait times predicted by the MTS model with .04 threshold noise (η = .04 in Equation 9). Bottom: scatter plot showing the predicted relation between IRI and wait time in the following interval.

lower than those predicted by the model. No previous theory has tackled all these results. Linear waiting (Wynne & Staddon, 1988) can duplicate temporal tracking but cannot account for gradual adjustment on step-up and step-down schedules or for the steady-state Weber law result, and, contrary to data, predicts high IRI versus wait-time correlations on VI schedules. The diffusion-generalization model (Staddon & Higa, 1991) can account for some

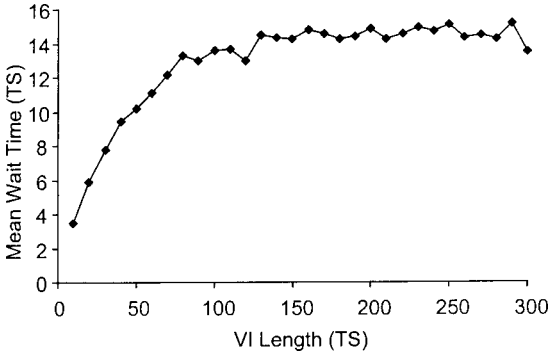

Fig. 12. Mean steady-state wait time predicted by the model for a range of random VI schedules from 10 to 200 time steps. Each point is the average of 1,000 intervals.

of these effects but fails to duplicate one-back tracking on cyclic and progressive schedules.

The fits to data in this paper are not typical of timing studies. Usually, an orderly but often highly averaged data set from a psychophysically based procedure, such as the peak-interval procedure, is fitted exactly by a model with perhaps five parameters (e.g., Gibbon & Church, 1990). We have approximated this procedure only for steady-state predictions (Figure 6). But for the dynamic predictions, we have attempted to match the organism's pattern of response to a wide range of dynamic interval procedures: impulse, step-up and step-down, sine-cyclic, and VI or RI schedules. In these cases, our aim is not so much to match the details of average performance as to match the range of performances of individual animals. To the extent that we have succeeded, the data from our simulations will not be readily distinguishable from data of the individual animals. Simulations of this sort cannot easily be subjected to statistics. Indeed, it is not at all clear just what statistics would be appropriate.

This method is not without risk. For example, suppose there is a series of numbers that is apparently random (but really derives from a chaotic process). Ignorance of the process means that such a series could not be distinguished from a random model—one apparently random series cannot readily be distinguished from another. But the random model does not in any sense predict or explain the series. This is reason to hesitate before adding a stochastic component to any model.

How parsimonious is our account? The full model has five parameters: M, the number of habituation units; parameter λ, which determines how the rate parameter a_j increases across units; b, the weighting that determines how the output of unit M contributes input to unit $M + 1$; ξ, the response threshold; and η, the additive noise term. Beyond a minimum of eight or so, the behavior of the model is not sensitive to the number of units. We have obtained adequate simulations with systems from 8 to 14 units. The noise parameter, η, is necessary only for the predictions of scalar timing (the CoV plot and distributions in Figure 6) and to reduce the correlation between IRI and wait time in the succeeding interval on VI (Figure 11). For most of the dynamic predictions, therefore, only three parameters need to be adjusted. In practice, we left b and ξ alone and simply explored variations in λ. The model has 14 state variables, which is more than scalar expectancy theory (two) but considerably fewer than Machado's (1997) model (60+). It is difficult to know what to make of these differences.

Limitations of the Model

The present model is deficient in at least three respects. First, it deals only with wait time. It says nothing about the pattern of responding after the first response in an interval. This limitation is shared with most steady-state timing theories: Scalar timing theory assumes an off-on-off pattern on the peak-interval procedure, for example, and hence cannot deal with FI scalloping, which is minimal after long training at short intervals but seems to persist at longer intervals (cf. Schneider, 1969; Staddon, 2001, pp. 317–319). One must choose where to begin, and wait time is perhaps the simplest, most direct (i.e., requiring the least averaging), and one of the most orderly measures of interval timing.

The second limitation is a consequence of the first: In its present single-threshold form, the model cannot deal with the concurrent timing of multiple intervals. On mixed FI FI schedules, for example, the response-rate distribution following each reinforcement often shows two peaks, corresponding to the two IRIs (e.g., Catania & Reynolds, 1968; Macha-

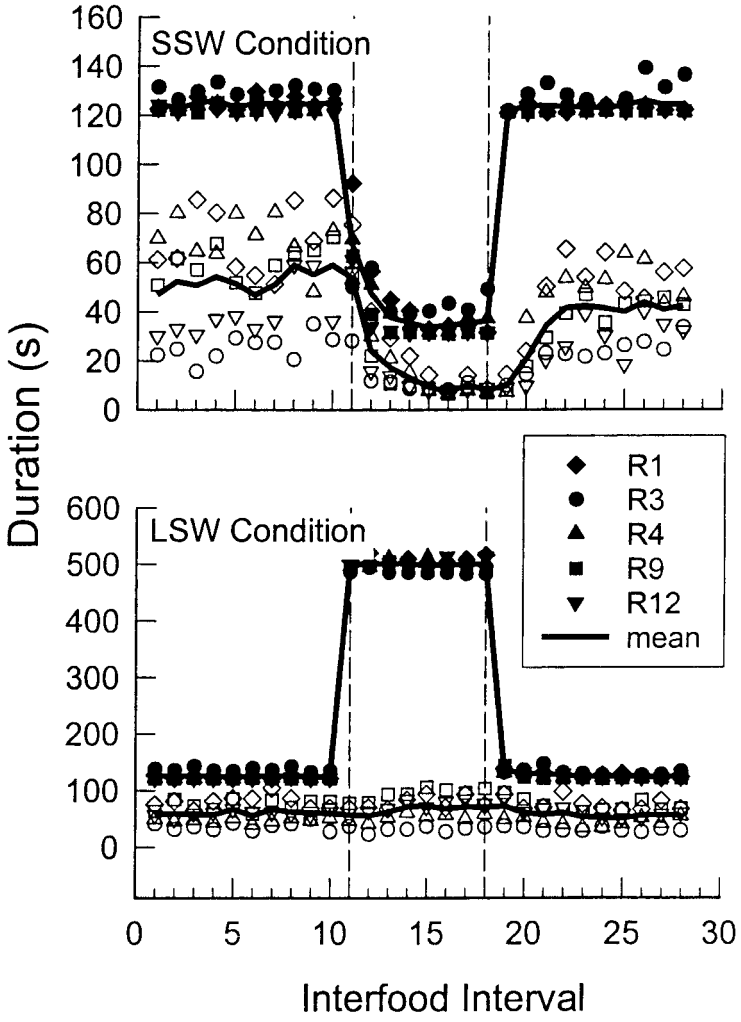

Fig. 13. Rats' mean wait time during a ''short square wave'' (SSW) in which IRIs changed one per session from 120 to 30 and back to 120 s and a ''long square wave'' (LSW) condition in which the IRIs changed from 120 to 480 and back to 120 s. Open symbols: data from individual rats; filled symbols show the actual IRI duration. Heavy solid lines: mean for all animals. Dashed vertical lines mark the start and end of a transition (from Higa & Staddon, 1997, Figure 10).

do, 1997). Nevertheless, as we mentioned earlier, with an additional assumption to allow responses after the first in each interval, the model can duplicate the qualitative features of responding on mixed FI schedules. The present model needs some additional assumptions—a ''stop'' as well as a ''start'' threshold, or some other provision to account for the effects of nonreinforcement as well as reinforcement—to duplicate these data in full quantitative detail.

Third, the model cannot account for the kind of dramatic failure to track shown in Figure 13. The figure is taken from Higa and Staddon (1997, Figure 10); it shows wait time in successive intervals on two schedules: a ''short square wave'' (SSW), in which IRIs changed once per session from 120 to 30 and back to 120 s, and a ''long square wave'' (LSW), in which the change was from 120 to 480 and back to 120 s. The animals (here rats) show the expected gradual tracking on the SSW condition (cf. with Figure 9, center panel, here) but completely fail to track the

long intervals in the LSW condition, a result that has also been obtained under chronic conditions with pigeons (Staddon, 1967). We are not sure whether this result is limited to the relatively long IRIs studied in this experiment. Some published data (Higa et al., 1991) and unpublished work in our laboratory suggest that animals may track when initially exposed to a mixed-interval schedule, but then cease tracking and settle down with short wait times after every reinforcer. In some cases, failure to track seems to reflect a persistent effect of a history that includes a high proportion of short intervals. It may, perhaps, be related to an earlier finding that short IRIs sometimes have more persistent effects than long ones do (Wynne & Staddon, 1992). A tendency to respond at a short postfood time necessarily preempts a tendency to respond at a later time, so that even a weak ''respond short'' tendency may override a stronger tendency to respond later. Our model assumes an instantaneous change in response threshold from IRI to IRI, but the preemption property of short times means that even a weak residual tendency to respond short may be sufficient to duplicate the effect shown in the bottom panel of Figure 13. Whatever the persistence differences between short versus long IRIs, they must be consistent with the apparently contrary fact that the effect of a *single* short IRI seems to be limited to the next interval (cf. Figures 2, 7, and 8).

There is a procedural asymmetry between step-down square-wave schedules, which pigeons and rats do track, and step-up schedules, which they do not. If the animal adjusts its wait time upwards during the long part of the LSW (short-long-short) series, it is likely to overshoot the first short interval when the short series resumes, that is, wait time may be longer than the programmed interval so that the animal responds after the reinforcer has set up. VI schedules, on which a very short interval may follow a long one, confront the organism with the same problem. Perhaps this overshooting, detected by the animal as immediate reinforcement of the first response in the interval, somehow energizes responding and shortens wait time in the succeeding intervals.

A process like this presumably depends on some experience with overshooting. Hence, we might expect to see much better tracking of IRI by wait time very early in an animal's exposure to a VI schedule. This is indeed what we found in the unpublished experiment by Higa described above. For the first 10 intervals of exposure to either an RI 15-s or an RI 60-s schedule, the correlations between obtained IRI (N) and wait time ($N + 1$) are shown in Table 1. All are positive and substantially larger than the correlations for the entire training period described earlier.

Table 1

Correlation between wait time and duration of preceding IRI on first exposure (first 10 IRIs) to random variable-interval 15 s or 60 s for 4 pigeons.

Bird	RI 15 s	RI 60 s
18[a]	.032	.472
299[a]	.524	.223
931[b]	.636	.374
174[b]	.213	.602

[a] Received VI 60 s then VI 15 s.
[b] Received VI 15 s then VI 60 s.

Despite these limitations, the wide range of data that are well fitted by the MTS timing model strongly suggests that two properties of the model—a slow process, which we have modeled as a tuned trace, and a rapid process, represented by instantaneous threshold setting by reinforcement—represent real characteristics of the interval-timing process.

REFERENCES

Baum, W. M. (1993). Performances on ratio and interval schedules of reinforcement: Data and theory. *Journal of the Experimental Analysis of Behavior, 59,* 245–264.

Catania, A. C., & Reynolds, G. S. (1968). A quantitative analysis of the behavior maintained by interval schedules of reinforcement. *Journal of the Experimental Analysis of Behavior, 11,* 327–383.

Church, R. M., & Lacourse, D. M. (1998). Serial pattern learning of temporal intervals. *Animal Learning & Behavior, 26,* 272–289.

Church, R. M., Meck, W. H., & Gibbon, J. (1994). Application of scalar timing theory to individual trials. *Journal of Experimental Psychology: Animal Behavior Processes, 20,* 135–155.

Dews, P. B. (1970). The theory of fixed-interval responding. In W. N. Schoenfeld (Ed.), *The theory of reinforcement schedules* (pp. 43–61). New York: Appleton-Century-Crofts.

Epstein, R. (1981). Amount consumed as a function of

magazine-cycle duration. *Behaviour Analysis Letters, 1,* 63–66.
Epstein, R. (1985). Amount consumed varies as a function of feeder design. *Journal of the Experimental Analysis of Behavior, 44,* 121–125.
Gibbon, J. (1977). Scalar expectancy theory and Weber's law in animal timing. *Psychological Review, 84,* 279–325.
Gibbon, J., & Church, R. M. (1990). Representation of time. *Cognition, 37,* 23–54.
Hatten, J. L., & Shull, R. L. (1983). Pausing on fixed-interval schedules: Effects of the prior feeder duration. *Behaviour Analysis Letters, 3,* 101–111.
Higa, J. J. (1996). Dynamics of time discrimination: II. The effects of multiple impulses. *Journal of the Experimental Analysis of Behavior, 66,* 117–134.
Higa, J. J., & Staddon, J. E. R. (1997). Dynamic models of rapid temporal control in animals. In C. M. Bradshaw & E. Szabadi (Eds.), *Time and behavior: Psychological and neurobiological analyses* (pp. 1–40). Amsterdam: Elsevier Science.
Higa, J. J., Wynne, C. D. L., & Staddon, J. E. R. (1991). Dynamics of time discrimination. *Journal of Experimental Psychology: Animal Behavior Processes, 17,* 281–291.
Killeen, P. R., & Fetterman, J. G. (1988). A behavioral theory of timing. *Psychological Review, 95,* 274–295.
Lejeune, H., Ferrara, A., Simons, F., & Wearden, J. H. (1997). Adjusting to changes in the time of reinforcement: Peak-interval transitions in rats. *Journal of Experimental Psychology: Animal Behavior Processes, 23,* 211–231.
Lowe, C. F., Davey, G. C., & Harzem, P. (1974). Effects of reinforcement magnitude on interval and ratio schedules. *Journal of the Experimental Analysis of Behavior, 22,* 553–560.
Machado, A. (1997). Learning the temporal dynamics of behavior. *Psychological Review, 104,* 241–265.
Meltzer, D., & Brahlek, J. A. (1970). Quantity of reinforcement and fixed-interval performance: Within-subject effects. *Psychonomic Science, 20,* 30–31.
Schneider, B. A. (1969). A two-state analysis of fixed-interval responding in pigeons. *Journal of the Experimental Analysis of Behavior, 12,* 667–687.
Staddon, J. E. R. (1965). Some properties of spaced responding in pigeons. *Journal of the Experimental Analysis of Behavior, 8,* 19–27.
Staddon, J. E. R. (1967). Attention and temporal discrimination: Factors controlling responding under a cyclic-interval schedule. *Journal of the Experimental Analysis of Behavior, 10,* 349–359.
Staddon, J. E. R. (1970). Effect of reinforcement duration on fixed-interval responding. *Journal of the Experimental Analysis of Behavior, 13,* 9–11.
Staddon, J. E. R. (2001). *Adaptive dynamics: The theoretical analysis of behavior.* Cambridge, MA: MIT/Bradford.
Staddon, J. E. R., & Higa, J. J. (1991). Temporal learning. In G. Bower (Ed.), *The psychology of learning and motivation* (Vol. 27, pp. 265–294). New York: Academic Press.
Staddon, J. E. R., & Higa, J. J. (1996). Multiple time scales in simple habituation. *Psychological Review, 103,* 720–733.
Staddon, J. E. R., & Higa, J. J. (1999). Time and memory: Towards a pacemaker-free theory of interval timing. *Journal of the Experimental Analysis of Behavior, 71,* 215–251.
Staddon, J. E. R., Higa, J. J., & Chelaru, I. M. (1999). Time, trace, memory. *Journal of the Experimental Analysis of Behavior, 71,* 293–301.
Staddon, J. E. R., Wynne, C. D. L., & Higa, J. J. (1991). The role of timing in reinforcement schedule performance. *Learning and Motivation, 22,* 200–225.
Wynne, C. D. L., & Staddon, J. E. R. (1988). Typical delay determines waiting time on periodic-food schedules: Static and dynamic tests. *Journal of the Experimental Analysis of Behavior, 50,* 197–210.
Wynne, C. D. L., & Staddon, J. E. R. (1992). Waiting in pigeons: The effects of daily intercalation on temporal discrimination. *Journal of the Experimental Analysis of Behavior, 58,* 47–66.
Zeiler, M. D., & Powell, D. G. (1994). Temporal control in fixed-interval schedules. *Journal of the Experimental Analysis of Behavior, 61,* 1–9.

Received November 20, 2000
Final acceptance September 23, 2001

APPENDIX

Steady-State Behavior of the MTS Model on FI Schedules

We suppose that after k_s fixed intervals the timing system has reached a steady state, so that trace value, $v(t)$ (Equation 6 in the text), is a periodic sequence:

$$v(kI + t) = v[(k+1)I + t],$$
$$t = 0, 1, \ldots, I - 1; \qquad k \geq k_s,$$

where k is an integer greater than k_s and I is FI length.

Computation of Periodic Inputs $X_i(I)$

In this section, we compute the values of the input signals $X_i(t)$ at the moment of reinforcement. When the time-marker signal (the cascade input X_1) is nonzero only at reinforcement, it is easy to prove that the inputs to later units, $X_i(t)$, are also nonzero only during reinforcement. In the steady-state regime, the integrator outputs V_i are periodic. We denote by $V_i(I)$ the value of the output V_i at the moment of reinforcement and by $M_i(I)$ the value of the output V_i in the time step just before reinforcement:

$$V_i[(k+1)I] = V_i(kI) = V_i(I)$$
$$V_i[(k+1)I-1] = V_i(kI-1) = M_i(I), \qquad k \geq k_s.$$

With this notation, and from Equation 5 at time $n = kI$,

$$V_i(kI) = a_i V_i(kI-1) + b_i X_i(kI),$$

one can infer that the inputs $X_i(t)$ are periodic in the steady-state regime

$$X_i[(k+1)I] = X_i(kI) = X_i(I),$$

because $V_i(I)$ and M_i are constant in time. From the previous theory and the integrator equation, we can write

$$V_i(I) = a_i M_i(I) + b_i X_i(I)$$
$$V_i(kI+I-1) = M_i(I) = a_i^{I-1} V_i(I).$$

After some algebraic manipulations, the relation among V_i, M_i, and X_i is

$$V_i(I) = \frac{b_i}{1-a_i^I} X_i(I)$$
$$M_i(I) = c_i(I) X_i(I),\ X(I),$$
$$C_i(I) = \frac{b_i a_i^{I-1}}{1-a_i^I}, \qquad i = 1, 2, \ldots, M.$$

From these equations and Equation 4, we can show using recursion that the unit inputs X_i in the steady-state regime are

$$X_i(I) = \begin{cases} \prod_{j=1}^{i-1} [1 - c_j(I)] X_1(I), \\ \quad \text{if } \forall j \ \ c_j(I) < 1 \\ 0, \quad \text{if } \exists j \ \ c_j(I) \geq 1, \\ \quad j = 1, 2, \ldots, i-1. \end{cases}$$

In our computer simulation we used a binary reinforcement sequence $X_1(I) = 1$. Input X_i is nonzero if every term $c_j(I)$, $j = 1, 2, \ldots, i-1$, is less than one. This might not be the case for some combination of a_j, b_j, and I. In such a case X_i is set to zero. Input $X_1(I)$ starts from zero [if any $c_j(I)$, $j = 1, 2, \ldots, i-1$, is greater than one], and increases monotonically to unit asymptote.

Computation of MTS Trace v

From Equation 5 in the steady-state regime,

$$V_i(kI) = a_i V_i(kI-1) + b_i X_i(kI)$$
$$V_i(kI+t) = a_i V_i(kI+t-1), \qquad t = 1, 2, \ldots, I-1, \qquad k \geq k_s$$

and the relations

$$V_i(I) = V_i(kI), \qquad M_i(I) = V_i(kI-1),$$
$$X_i(I) = X_i(kI),$$

we can write

$$V_i(I) = a_i M_i(I) + b_i X_i(I)$$
$$V_i(kI+1) = a_i V_i(I),$$
$$V_i(kI+t) = a_i^t V_i(I), \qquad t = 1, 2, \ldots, N-1.$$

The trace signal, $v(t)$, is computed as the sum of integrator outputs V_i

$$v(kI+t) = \sum_{i=1}^{M} V_i(kI+t) = \sum_{i=1}^{M} V_i(I)\, a_i^t, \qquad k \geq k_s, \qquad t = 0, 1, \ldots, I-1.$$

The numbers $V_i(I)$, defined at $V_i(I) = V_i(kI)$, $k \geq k_s$, represent the integrator outputs at the instant of reinforcement. From the above equations it follows that values $V_i(I)$ are

$$V_1(I) = \frac{b_1}{1-a_1^I} X_1(I)$$
$$V_i(I) = \begin{cases} \frac{b_i}{1-a_i^I} \prod_{j=1}^{i-1} [1 - c_j(I)] X_1(I), \\ \quad \text{if } \forall j \ \ c_j(I) < 1 \\ 0, \quad \text{if } \exists j \ \ c_j(I) \geq 1, \\ \quad i = 2, 3, \ldots, M \end{cases}$$
$$c_j(I) = \frac{b_j a_j^{I-1}}{1-a_j^I}.$$

Thus, $V_i(I)$ starts with a value of zero, increases to a maximum, and declines to an asymptote of value b_i.

Computation of Reinforcement Memory (RFM)

Reinforcement memory is just the remembered value of the trace at the instant of reinforcement: v_{rft}. The value of RFM is

$$\begin{aligned}\mathrm{RFM}(t+1) &= \mathrm{RFM}(t) + X_1(t)[v(t-1) + \eta\epsilon(t) \\ &\qquad - \mathrm{RFM}(t)],\end{aligned}$$

where $X_1(t)$ is the reinforcement sequence, v is the trace value, $\epsilon(t)$ is a noise series with zero mean and unit dispersion, and η is a constant (see Equation 9).

In the steady-state regime we have

$$\begin{aligned}\mathrm{RFM}(kI) &= v(kI-1) + \eta\epsilon(kI) \\ \mathrm{RFM}(kI+t) &= \mathrm{RFM}(kI), \\ t &= 1, 2, \ldots, I-1, \qquad k \geq k_s.\end{aligned}$$

Using the previous notation, one can write the RFM signal as

$$\begin{aligned}\mathrm{RFM}(kI) &= \sum_{i=1}^{M} M_i(I) + \eta\epsilon(kI) \\ \mathrm{RFM}(kI+t) &= \mathrm{RFM}(kI), \\ t &= 1, 2, \ldots, I-1.\end{aligned}$$

The RFM signal is constant between reinforcements and is a stochastic variable at the moment of reinforcement. RFM mean is equal to the sum of the numbers $M_i(I) = V_i(kI-1)$, $k \geq k_s$, because $\epsilon(t)$ has a mean equal to zero

$$\begin{aligned}E[\mathrm{RFM}(t)] &= E\left[\sum_{i=1}^{M} M_i(I)\right] + E[\eta\epsilon(t)] \\ &= \sum_{i=1}^{M} M_i(I).\end{aligned}$$

A number $M_i(I)$, representing the value of output V_i before reinforcement, starts with a value of zero, increases to a maximum, and decreases to an asymptote of zero. The values of $M_i(I)$ are given by

$$M_1(I) = c_1(I)X_1(I)$$

$$M_i(I) = \begin{cases} c_i(I)\displaystyle\prod_{j=1}^{i-1}[1 - c_j(I)]X_1(I), \\ \quad \text{if } \forall j \;\; c_j(I) < 1 \\ 0, \quad \text{if } \exists j \;\; c_j(I) \geq 1, \\ \quad i = 2, 3, \ldots, M \end{cases}$$

$$c_j(I) = \frac{b_j a_j^{I-1}}{1 - a_j^I}.$$